DISCOVERIE

Project No. 848228

DISCOvERIE

Development, dIagnostic and prevention of gender-related Somatic and mental COmorbitiEs in iRritable bowel syndrome In Europe

Workpackage 3
Deliverable D3.3
Intestinal mucosal profiling of mechanisms of barrier dysfunction that differentiate IBS from comorbid IBS

Start date of project: 2020-01-01

End Date: 2024-12-31

Duration: 60 months

Organisation name of lead contractor for this deliverable:

Partner 1 (VHIR): Fundacio Hospital Universitari Vall d'Hebron- Institut de Recerca

Project co-funded by the European Commission within the Horizon 2020 research and innovation programme under Grant Agreement No 848228		
Dissemination Level		
PU	Public	
PP	Restricted to other programme participants (including the Commission Services)	
RE	Restricted to a group specified by the consortium (including the Commission Services)	
CO	Confidential, only for members of the consortium (including the Commission Services)	X

Disclaimer

Consortium

Partcicipant Nº	Participant Legal Name	Country	Partner's Acronym
1	Fundacio Hospital Universitari Vall d'Hebron-Institut de recerca	ES	VHIR
2	Goeteborgs Universitet	SE	UGOT
4	University College Cork – National University of Ireland, Cork	IE	UCC
5	Johann Wolfgang Goethe – Universitatfrankfurt Am Main	DE	GUF
6	Katholieke Univeriteit Leuven	BE	KUL
7	Universitatsklinikum Heidelberg	DE	UKL-HD
8	Alma Mater Studiorum – Universita Di Bologna	IT	UNIBO
9	VIB VZW	BE	VIB
10	Universiteit Maastricht	NL	UM
11	Semmelweis Eguetem	HU	SU

12	Universitatea de Medicina Si Farmacie Iuliu Hatieganu Cluj-Napoca	ROU	UMF
13	Anaxomics Biotech, S.L.	ES	AX
14	Hycult Biotechnology BV	NL	HB
15	Emergentec Biodevelopment GMBH	AU	EMTEC
16	Nanostring Technologies Inc	USA	NSTG
17	Cliclab Technologies Inc	ES	Cliclab
18	Followhealth SL	ES	hITc
19	BYTE Factory Systems SL	ES	BF
20	Stichting Radboud Universitair Medisch Centrum	NL	RUMC

Table of Contents

LIST OF ABBREVIATIONS

AUC: Area under the receiver operating characteristic curve

DAB: 3,3'-¬Diaminobenzidina

DE: Differentially expressed

DGBI: Disorder of gut-brain interaction

FITC: Fluorescein-5-(and-6)-Sulfonic Acid

DMEM. Dulbecco's modified Eagle's medium

F: Female

FBS: Fetal bovine serum

FDR: False discovery rate

GAP43: Growth associated protein 43

HV: Healthy volunteers

HIER: Heat-induced epitope retrieval

Hpf: High power field

IBS: Irritable Bowel Syndrome

IBS-A: IBS alone

IBS-Co: IBS comorbid

IBS-Mco: IBS multicomorbid

IF: Immunofluorescence

IHC: Immunohistochemistry

JAM-A: Junctional adhesion molecule-A

LCMS: Proteomic analysis by liquid chromatography mass spectrometry

M: Male

MC: Mast cell

NA: not applicable

PFA: Paraformaldehyde

PB: Phosphate buffer

qPCR: Real time PCR

RT: Room temperature

TEM: Transmission electron microscopy

TER: Transepithelial cell resistance

TJ: Tight junction

VST: Variance-stabilizing transformation

WP: Work package

WB: Western blot

ZO: Zonula occludens

LIST OF FIGURES

LIST OF TABLES

1. Executive Summary

Background: Irritable bowel syndrome (IBS) is characterized by chronic and recurrent abdominal pain and altered bowel habits. Although the origin of IBS seems to be multifactorial and is still not well defined, dysfunction of the intestinal epithelial barrier is now recognized as one of the main mechanisms involved in IBS pathophysiology. Intestinal barrier dysfunction, has been associated to several extra digestive conditions including depression and fibromyalgia, among others.

Aim: to evaluate how mental and somatic disorders affect the intestinal barrier in IBS.

Methods: Mucosal biopsies obtained in WP2 were analysed through transcriptomic and proteomic approaches to describe the molecular profile in IBS and IBS associated to mental and somatic comorbidities. Immune mucosal populations and enteric nerve fibers involved in neuro-plastic changes were characterized by immunohistochemistry. An ultrastructural analysis of mucosal mast cells, with a specific focus on mast cell degranulation was performed.

Results: Transcriptomic and proteomic analysis of colonic biopsies revealed several proteins differentially expressed between IBS and IBS associated to mental and somatic comorbidities. GAP43 positive fibres were increased in IBS comorbid and multicomorbid groups compared to HC, in association with higher mast cell degranulation in these IBS groups.

Conclusion: mental and somatic comorbidities in IBS patients are associated with different molecular, cellular and ultrastructural profiles. However, validation experiments need to be performed to confirm these results.

2. Introduction

Irritable bowel syndrome (IBS) is a disorder of gut-brain interaction (DGBI) characterized by chronic and recurrent abdominal pain and altered bowel habits. Although the origin of IBS seems to be multifactorial and is still not well defined, dysfunction of the intestinal epithelial barrier is now recognized as one of the main mechanisms involved in IBS pathophysiology[1]. Intestinal barrier function is essential to maintain gut mucosal homeostasis, as the gastrointestinal tract is continuously exposed to enormous amounts of luminal antigens that need to be processed. In this regard, intestinal barrier has the unique ability to allow nutrient digestion and absorption, but at the same time, preventing potentially harmful substances from reaching the inner environment, while allowing the selective passage of substances contributing to the development of the intestinal immune system and immune tolerance. The breakdown of intestinal epithelial barrier's surveillance might facilitate unfettered penetration of food and microbial antigens across the epithelial barrier leading to an inappropriate immune stimulation and favouring the development of mucosal inflammation. Therefore, the loss of intestinal barrier integrity may have a pivotal role in the onset and progression of several gastrointestinal and non-gastrointestinal diseases. In fact, increased intestinal permeability, as an indicator of intestinal barrier dysfunction, has been associated to several extra digestive conditions including obesity, diabetes mellitus[2], atopic or allergic diseases[3], and most importantly, depression[4] and fibromyalgia[5], among others.

Work package (WP) 3 aims to functionally and structurally evaluate how mental (such as depression, anxiety) and somatic (such as chronic fatigue, fibromyalgia) disorders affect the intestinal barrier function in IBS and includes four tasks:

T3.1) Intestinal barrier permeability assessment in patients and controls.

T3.2) Intestinal barrier permeability assessment in preclinical models.

T3.3) Molecular, cellular and ultrastructural characterization of the intestinal mucosa.

T3.4) Immune, neural and luminal-derived mechanisms of epithelial dysfunction.

This deliverable 3.3 explains the work performed in tasks 3.3 and 3.4.

3. Methods and Results

4.1. TASK 3.3) Molecular, cellular and ultrastructural characterization of the intestinal mucosa (VHIR, UNIBO, KUL, UGOT, AX)

In this task, we aim to investigate the cellular and molecular profiles that differentiate IBS and associated comorbidities. For this purpose, colonic mucosal biopsies have been collected from subjects recruited in WP2 and have been processed for further analysis (n=174, Table 1). Due to the COVID-19 pandemics, enrolment of patients into de DISCOvERIE project and, most importantly, collection of biopsies was severely delayed as endoscopy units were forced to cancel or significantly reduce all elective endoscopic procedures. As a result, subject recruitment was severely delayed; fewer colon biopsies were collected, and later than originally planned. However, most centres almost reached the colonic biopsies targets.

From each subject, sixteen biopsies +/- 3 (in case Ussing Chambers experiments were performed at KUL and VHIR for task 3.1) +/- 2 (in case optional samples for microbiota analysis were collected for WP5) were taken from the descending colon and preserved as shown in table 2.

Table 1 - Summary of colonic biopsies collected.

COLONIC BIOPSIES	VHIR	KUL	UGOT	UNIBO	UM	UMF	Total
IBS alone	8	4	13	12		17	54
IBS comorbid (IBS+mental)	9	1	20	10		9	49
IBS comorbid (IBS+somatic)		1		2		1	4
IBS Multicomorbid	11	0	6	3	1	3	24
Only Mental							0
Only Somatic							0
Somatic+mental							0
Healthy control	24	11	8				43
Total	52	17	47	27	1	30	174

Table 2 - Preservation of colonic biopsies collected.

Technique	**Shipment to**	**Number of biopsies**	**Preservation**	**Site**
Transcriptomics and qPCR	VHIR	2 (1 tube)	RNA later -80ºC	Descending colon
Proteomics and WB	VHIR UNIBO	3 (1 tube) 2 (1 tube)	Snap frozen -80ºC Snap frozen -80ºC	Descending colon
IF and IHC	VHIR UNIBO	2 (1 tube) 2 (1 tube)	buffered 10% formalin buffered 10% formalin	Descending colon
Electron micoscopy (TEM)	VHIR	1 (1 tube)	2%PFA+2.5%Gluta	Descending colon
Ussing Chambers	NA	3	NA	Descending colon
Supernatants	UNIBO	4 (1 tube)	-80ºC	Descending colon
Gut microbiome (optional, if possible)	VIB	2 (2 tubes; 1/tube)	Snap frozen -80ºC	Descending colon

qPCR: real time PCR; WB, western blot; IF, immunofluorescence; IHC, immunohistochemistry; TEM, transmission electron microscopy, NA, not applicable.

4.1.1 Molecular characterization of the intestinal mucosa

To perform molecular transcriptome/proteome profiling for further identification of distinctive biological functions and active molecular pathways specific of IBS and associated mental and somatic comorbidities, we selected 80 subjects as follows:

- 20 subjects from the IBS alone group.

- 20 subjects from the IBS comorbid group (mental comorbidities).

- 20 subjects from the IBS multicomorbid group.

Sex, age and IBS subgroup (diarrhoea, constipation, mixed and undefined) were equilibrated in each group if possible. One subject was excluded from the analysis as she turned to be an IBS patient instead of healthy subject. Female sex was predominant in all IBS groups, particularly in the IBS multicomorbid, with higher proportion of females (p=0.048, Table 3).

Table 3 - Sex distribution between groups.

			Sex	
			Female	Male
PATIENT GROUP	IBS ALONE	Recuento	11	9
		% dentro de PATIENT GROUP	55,0%	45,0%
	IBS COMORBID	Recuento	14	6
		% dentro de PATIENT GROUP	70,0%	30,0%
	IBS MULTICOMORBID	Recuento	18	2
		% dentro de PATIENT GROUP	90,0%	10,0%
	HEALTHY SUBJECTS	Recuento	9	10
		% dentro de PATIENT GROUP	47,4%	52,6%
Total		Recuento	52	27
		% dentro de PATIENT GROUP	65,8%	34,2%

There were no differences in age between patient's group in terms of age (p=0.073), smoking habit (p=0.677), alcohol consumption (p=0.799), IBS subtype (p=0.448).

A. Transcriptomics and Proteomics methodology

Transcriptomic analysis by RNAseq

RNA extraction: Colonic biopsies (HV n=19 (9F:10M), IBS alone n=20 (11F:9M), IBS comorbid n=20 (14F:6M), IBS multicomorbid n=20 (18F:2M) previously preserved in RNA later, have been processed for RNA extraction using the Rneasy Mini Kit using the Buffer Tissue Lyser II and performing RNase/DNase treatment. Sample processing was performed according to the manufacturer's instructions. The quality of all assayed RNAs (RNA integrity characterization) was evaluated by Agilent RNA 6000 Nano Chips (Agilent Technologies, Cat# 5067-1511), respectively. Only samples with values of RIN ≥7 were included in the analysis, from which 11-13 subjects from each group were blindly selected for RNA-seq analysis.

RNAseq analysis: Sequencing libraries were prepared following "True Stranded mRNA Sample Preparation Guide (Part # 15031058 Rev. E)" using the "TrueSeq Stranded mRNA Library Prep" kit (Illumina Inc. Cat #20020594) and TruSeq RNA CD Index Plate (96 Indexes, 96 Samples) (Illumina Inc. Cat #200191792), Starting from 600 ng of total RNA, mRNA was purified, fragmented and primed for cDNA synthesis. cDNA first strand

was synthesized with SuperScript-II Reverse Transcriptase (Thermo Fisher Scientific, Cat #18064-014) for 10 min at 25°C, 15 min at 42°C, 15 min at 70°C and pause at 4°C. cDNA second strand was synthesized with Illumina reagents at 16°C for 1 hour. Then, A-tailing and adaptor ligation were performed. Finally, enrichment of libraries was achieved by PCR (30 sec at 98°C; 15 cycle of 10 sec at 98°C, 30 sec at 60°C, 30 sec at 72°C, 5 min at 72°C and pause at 4°C. Afterwards, libraries were visualized on an Agilent 2100 Bioanalyzer using Agilent High Sensitivity DNA kit (Agilent Technologies, Cat #5067-4626) and quantified using Qubit dsDNA HS DNA Kit (Thermo Fisher Scientific, Cat #Q32854). Obtained libraries had the expected size and its concentration was appropriate for sequencing, Illumina SBS technology has been used to sequencing (NOvaSeq 6000) the libraries, obtaining at least 100 million paired end reads of 100 nucleotides (50 million reads for Read1 and 50 million reads for Read2). Sequencing data is converted into raw data for the analysis (FASTQ).

Proteomic analysis by liquid chromatography mass spectrometry (LCMS)

Colonic biopsies from HV n=14 (7F:7M), IBS alone n=15 (8F:7M), IBS comorbid n=15 (9F:6M) and IBS multicomorbid n=15 (13F:2M) have been included in the proteomics study. Protein extraction has been carried out from all samples by sonication in 500 µl of buffer 30 mM Tris.HCL, 7 M Urea, 2 M Thiourea, 4% CHAPS, after centrifugation 1/5 part of the extract was purified by precipitation with TCA/acetone. The purified protein pellet was resuspended in 50 mM ammonium bicarbonate, 6 M Urea and digested with trypsin. Tryptic digests were purified on a ZipTrip reverse phase microcolumn prior to LCMS analysis. LCMS analysis was performed with a 120 min gradient (one run of LCMS per samples), without labelling, in the Orbitrap Eclipse spectrometer of the CRG. A quantitative proteomic analysis has been carried out using the label-free Proteome Discoverer 2.5 (Thermo) analysis software and has allowed the identification and quantitative comparison of around 6600 proteins.

B. Transcriptomics and Proteomics Results

RNA-Seq differential expression analysis of IBS patients

Differential expression analyses of all pairwise comparisons between the healthy control, alone, comorbid and multicomorbid IBS patients were done with DESeq2[6]. Additional

differential expression analyses were done segmenting by IBS type diarrhea and biological sex (male and female). An FDR value less than 0.05 was used as threshold to identify differentially expressed (DE) genes.

Significant DE genes were only observed by selecting IBS patient suffering from diarrhoea (see **Table 4**). **Figure 1**).

***Table 4* - Number of DE genes observed in the pairwise comparisons between the healthy and IBS cohorts.**

A larger number of DE genes corresponding to gender-related genes were identified in the analyses of multicomorbid patients without gender stratification due to the high imbalance of female patients in the multicomorbid diarrhoea patients. Besides the gender-related genes, two other genes named Gene A and Gene B were seen as DE in several comparisons. Gene A was DE in both IBS diarrhoea vs healthy patients, whereas Gene B was seen as DE in the IBS-alone diarrhoea vs healthy female patients, IBS alone vs comorbid diarrhoea male patients and IBS multicomorbid diarrhoea vs healthy female patients. Both genes showed differences in their expression between the IBS subtypes and between male and female patients (see **Figure 1**).

***Table 4* - Number of DE genes observed in the pairwise comparisons between the healthy and IBS cohorts.**

Analyses that identified any DE genes are only shown. D denotes IBS patients suffering from diarrhoea in the IBS type column. M and F denote male and female patients in the Sex column, respectively.

Comparison	IBS type	Sex	Number of DE expressed genes
Alone vs Comorbid	D	M	1
Alone vs Multicomorbid	D	All	9
Alone vs Healthy	D	All	1
Alone vs Healthy	D	F	2
Multicomorbid vs Comorbid	D	All	4
Multicomorbid vs Healthy	D	All	8
Multicomorbid vs Healthy	D	F	1

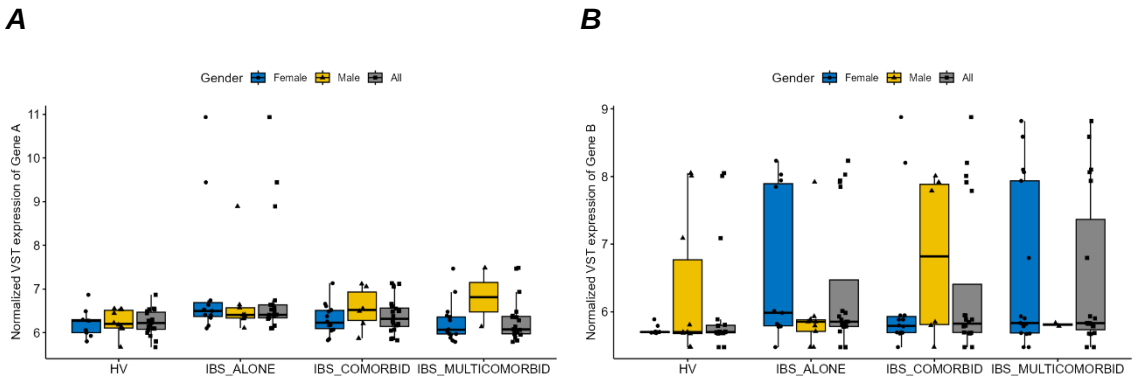

Figure 1 Boxplots of the normalized expression of gene A (A) and gene B (B) in the IBS subtypes, separated by male and female patients.

Proteomics differential expression analysis of IBS patients

The differential expression analyses of all the pairwise comparisons between the IBS cohorts and the healthy samples were performed using *limma*[7]. In each comparison, proteins that were expressed in at least two samples in each class were considered. An FDR value of 0.05 was set as threshold to identify differentially expressed proteins. In addition, DE proteins were mapped to genes using the same gene-protein relation defined for the RNA-Seq data.

The number of DE proteins seen in the 6 comparisons between the IBS cohorts and healthy samples are shown in **Table 5**. Among the 8 DE proteins seen in the alone vs healthy comparison, only one, protein A, was seen as DE in the alone vs comorbid comparison. Interestingly, 3 proteins; proteins B, C and D, were identified as DE in the comorbid vs healthy and comorbid vs alone comparisons (see **Figure 2**).

Two of them, proteins C and D, were also DE in the comorbid vs multicomorbid analysis, giving them a potential diagnostic role for the IBS-comorbid cohort. In addition, protein E was identified as DE in the comorbid vs alone and multicomorbid vs comorbid comparisons, but no significant difference was seen in the comparisons of comorbid patients with the healthy ones. As for the multicomorbid patients, despite having the largest number of DE proteins in the healthy comparison, only three proteins, proteins F, G and H, was seen both as DE in the healthy and comorbid comparisons (see **Figure 4**).

The single protein seen as DE in the multicomorbid vs alone comparison was protein I.

Table 5 - Number of DE proteins seen in the pairwise comparisons between the IBS cohorts and healthy patients.

Comparison	Number of DE expressed proteins
Alone vs Healthy	8
Comorbid vs Healthy	25
Multicomorbid vs Healthy	129
Comorbid vs Alone	6
Multicomorbid vs Alone	1
Multicomorbid vs Comorbid	10

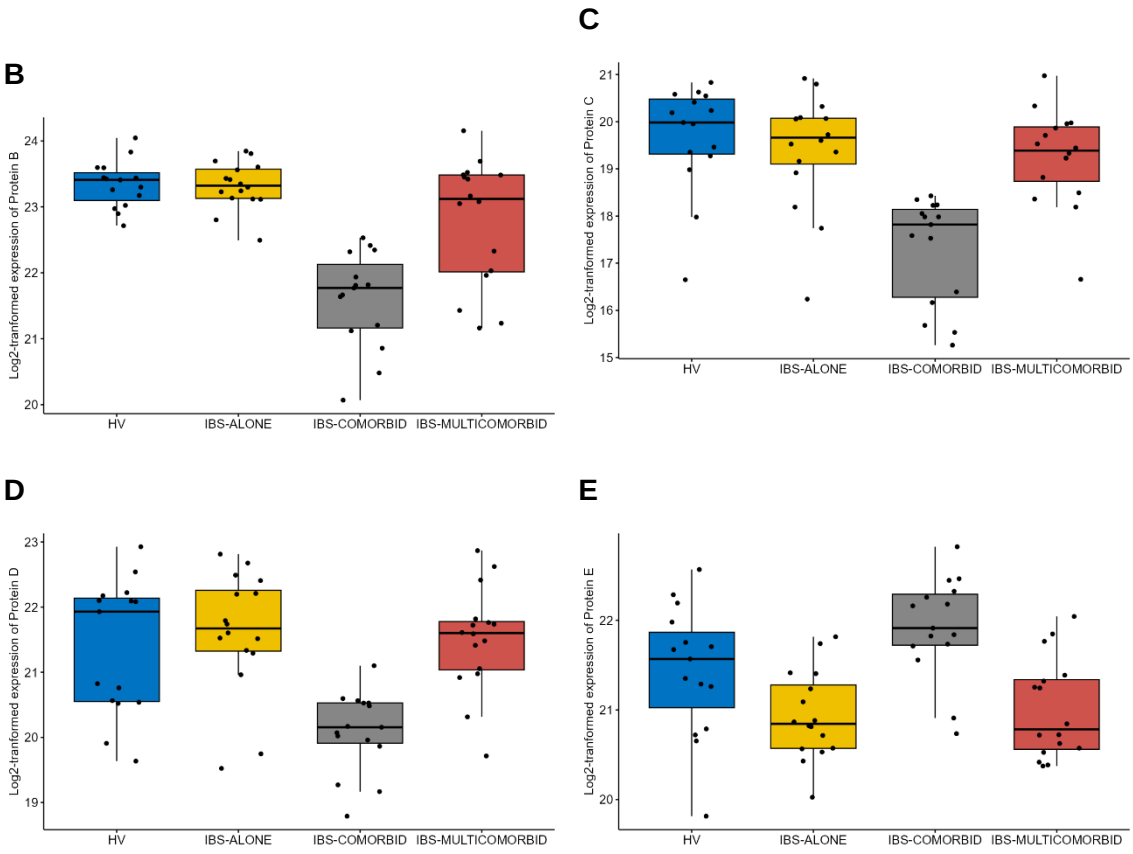

Figure 3 Boxplots of the DE proteins B (B), C (C), D (D) and E (E), with a high diagnostic ability of the IBS-comorbid cohort.

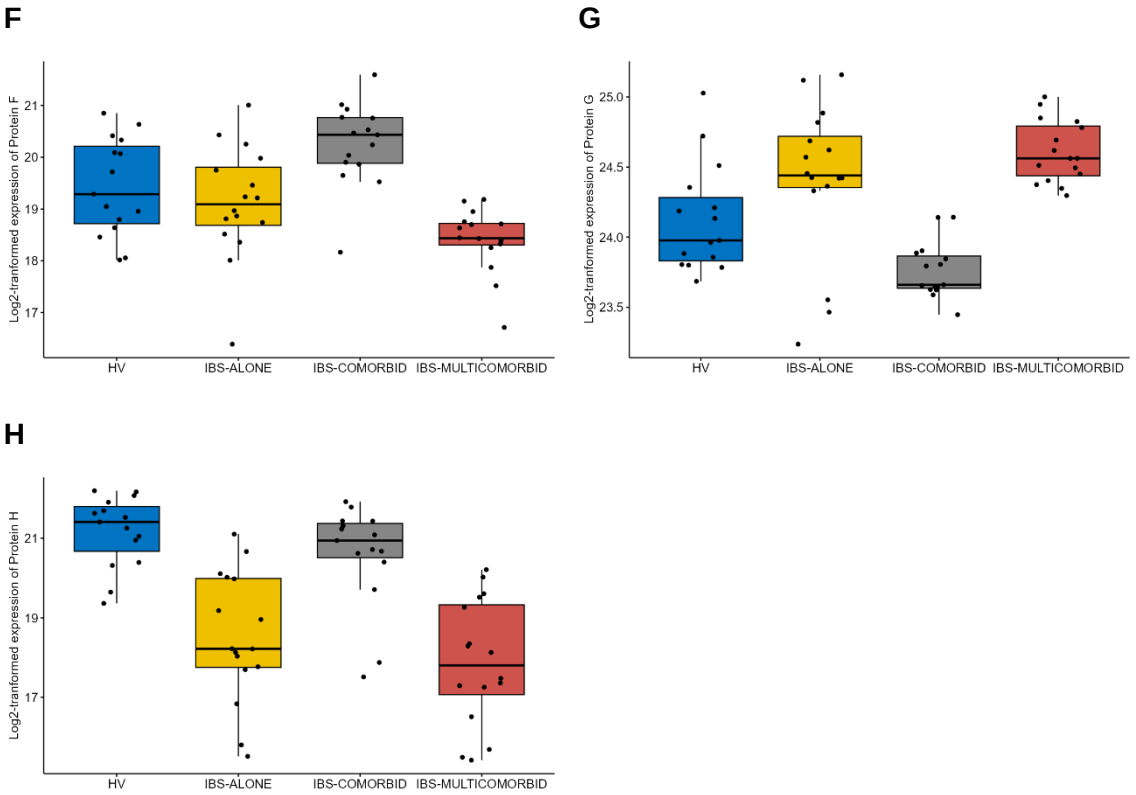

Figure 4 - Boxplots of the DE proteins F (F), G (G) and H (H), with a high diagnostic ability of the IBS-multicomorbid cohort.

Univariate linear model analysis of IBS patients' transcriptome and proteome

Univariate linear models of genes and proteins corresponding to the pairwise comparisons between the IBS cohorts and healthy patients were built using the gene and protein expression data obtained from the IBS and healthy patients. VST-normalized gene expression and log2-tranformed protein expression data were used to build the gene and protein univariate models. A gene or protein was deemed significant if the Area Under the Receiver Operating Characteristic Curve (AUC) was greater or equal to 0.7 after a 10-fold cross-validation. Gene and proteins with significant diagnostic ability were determined as those seen as significant against the healthy and remaining IBS cohorts' comparisons.

The number of genes with an AUC value greater or equal to 0.7 are shown in **Table 7.**

Table 6 - Number of significant genes obtained from the univariate logistic regression models for the 6 pairwise comparisons.

Unlike the differential expression analysis, a larger number of genes with diagnostic potential of the different IBS cohorts were observed. Only one gene (gene A) significant

in the IBS alone vs healthy logistic regression model was also seen as DE in the RNA-Seq data analysis, highlighting its potential diagnostic utility for IBS-alone (see **Figure 1**).

Table 6 - Number of significant genes obtained from the univariate logistic regression models for the 6 pairwise comparisons.

The numbers in the 3rd column denote the number of significant genes seen in both the corresponding healthy and remaining IBS cohorts' comparisons for each IBS cohort**.**

Comparison	Number of significant genes	Number of significant IBS cohort genes
Alone vs Healthy	158	10
Alone vs rest IBS	95	
Comorbid vs Healthy	390	33
Comorbid vs rest IBS	90	
Multicomorbid vs Healthy	419	62
Multicomorbid vs rest IBS	234	

Despite having identified fewer proteins with expression, a large number of proteins with diagnostic potential were observed from the univariate models, similar to the results seen for the univariate gene expression models (see **Table 6**).

Table 7 - Number of significant proteins obtained from the univariate logistic regression models for the 6 pairwise comparisons.

Comparison	Number of significant proteins	Number of significant IBS cohort proteins
IBS-alone vs Healthy	158	14
IBS-alone vs rest IBS	229	
IBS-comorbid vs Healthy	614	45
IBS-comorbid vs rest IBS	120	
IBS-multicomorbid vs Healthy	1099	143

IBS-multicomorbid vs rest IBS	222	

Fourteen proteins were found as potential diagnostic biomarkers of the IBS-alone cohort. Among those significant protein, three proteins (proteins I, J and K) were also seen as DE in the alone vs healthy differential expression analysis of proteomics data (see **Figure 5**).

Protein I was also seen as DE in the multicomorbid vs alone differential expression comparison using the proteomics data. Similar to protein I, an additional protein identified by the logistic models, protein L, was seen as DE in the same comparison. None of these proteins were found as DE or significant in the RNA-Seq data analysis.

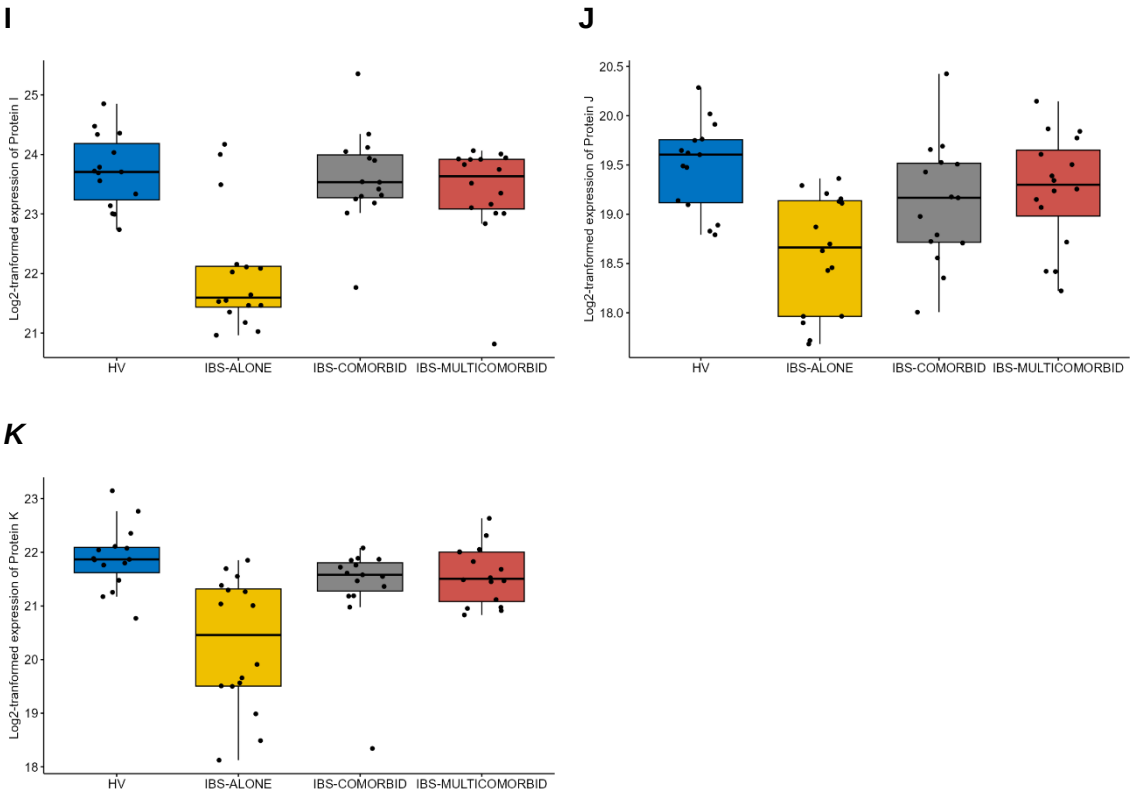

Figure 5 - Boxplots of the significant proteins I (I), J (J) and K (K), identified as those with a high potential diagnostic of the IBS-alone cohort.

Proteins C and D were found among the 45 proteins representative of comorbid IBS patients identified by the logistic models (see **Figure 3**).

Protein B identified as DE in the comorbid vs alone and comorbid vs healthy comparisons of the proteomic differential expression analysis (see **Figure 3)**.

Similar to the IBS-comorbid cohort results, the three proteins highlighted as potential diagnostic biomarkers of the IBS-multicomorbid cohort in the proteomics differential expression analysis; proteins F, G and H, were found among the 143 significant proteins given by the logistic models. Nevertheless, none of these proteins were found in the equivalent analyses done in the RNA-Seq data.

4.1.2 Cellular characterization of the intestinal mucosa

We performed quantitative immunohistochemistry on paraffin-embedded biopsies collected from WP2.

A. Quantification of mast cells, eosinophils and GAP43 positive fibers in the colonic mucosa

At UNIBO, we focused on the quantification of mast cells, eosinophils and sprouting fibers.

Paraffin-embedded biopsies were cut at 3-4 µm using a microtome. Mast cells were detected by using an antibody against tryptase, eosin staining was used to detect eosinophils, while nerve sprouting, defined as the outgrowth of new nerve fibres, was detected by growth associated protein 43 (GAP43) staining. Stained cells/fibres were quantified in blind fashion and using a computer-assisted analysis system (ImageJ Software). Results are expressed as percentage of cells/fibres over *lamina propria* area (mm2). The samples analysed were matched to those used for the transcriptomic analyses, with the aim of characterizing the samples as far as possible for future correlation analyses.

As shown in Figure 5, mast cells are increased only in patients with IBS alone compared to HC, although without reaching the statistical significance (Fig. 5A). Eosinophils are slightly increased in the three IBS groups, but again we did not find any statistical significance (Fig. 5B). Interestingly, GAP43 positive fibres were increased in the three IBS subgroups compared to HC and this increase was significant in the IBS comorbid and multicomorbid groups compared to HC (Fig. 5C).

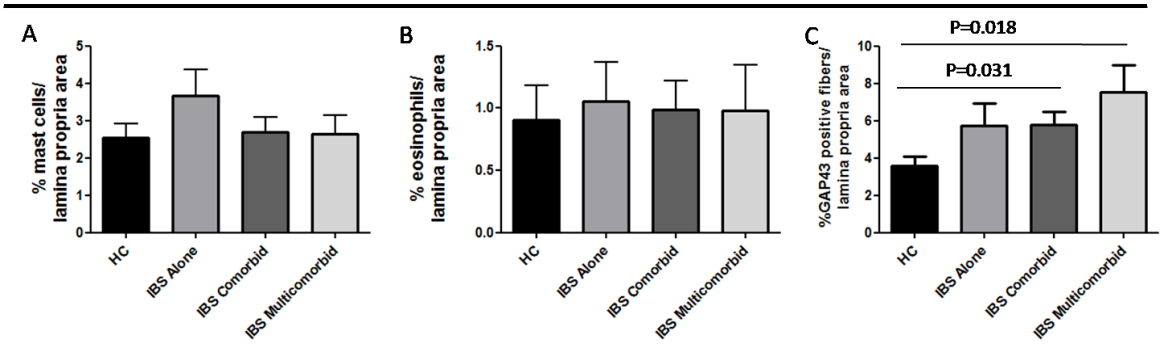

Figure 6 - Quantification of mast cells, eosinophils and GAP43 positive fibers in the colonic mucosa.
A: mast cells in the colonic mucosa, HC:14, IBS alone: 18, IBS comorbid: 18, IBS multicomorbid: 9. B: eosinophils in the colonic mucosa, HC:16, IBS alone: 16, IBS comorbid: 23, IBS multicomorbid: 10. C: sprouting fibers in the colonic mucosa, HC:9, IBS alone:7, IBS comorbid: 7, IBS multicomorbid: 6.

The analysis of these results according to clinical manifestations (in particular abdominal pain score) and to the presence of allergy, will clarify the role of these two immune cell populations and sprouting events in IBS with and without comorbidities. To evaluate neuro-immune interactions, double staining experiments were performed to assess the number of mast cells/eosinophils close (less than 5µm) to GAP43 positive fibres, and we are currently analysing these results.

B. Quantification of mast cells and mast cell degranulation in the colonic mucosa

At VHIR, we focused on the quantification of mast cells in the epithelium and lamina proprio, but also in mast cell degranulation in the different IBS groups.

Colonic mucosal tryptase+ mast cell

A total of 10 HV subjects and 29 IBS patients were included in order to assess colonic mucosal tryptase$^+$ mast cell counts and activation. The IBS group included 9 IBS-Alone patients, 10 IBS-Comorbid patients and 10 IBS-multicomorbid patients.

Colonic biopsies included in paraffine blocks were cut at 4 µm, placed onto slides, deparaffinized, and rehydrated following general procedures. Heat-induced epitope retrieval (HIER) method was performed by heating the samples (dipped in citrate buffer pH=6) at 120ºC in an autoclave for 10 minutes.

Endogenous peroxidase blocking was carried out by incubating the tissue samples with Peroxidase Blocking solution for 10 minutes. Next, non--specific sites were blocked with Protein Block solution (Agilent®, ref:X0909) for 15 minutes. Next, samples were incubated with mouse anti-Human Mast cell Tryptase primary antibody (1/200; DAKO) for 30 minutes, followed by another 30-minute incubation with anti-mouse secondary antibody (EnVision+System-HRP, DAKO). Later, the samples were incubated with a solution of 3,3'--Diaminobenzidina (DAB) Chromogen and Substrate Buffer. Mast cell infiltration was determined by counting the total number of Tryptase+ cells present both in lamina propria and inside the epithelium. Positive cells were counted by high power field (hpf) at 400x magnification using a Leica DMLB optical microscope (Leica Microsystems GmbH). In parallel, the tryptase-stained area in lamina propria was quantified by QuPath (version 0.4.3), a bioimage analysis software. Digital scans of the IHC were obtained from the Department of d'Anatomia Patològica de l'Hospital Vall d'Hebron (Barcelona).

In all groups, tryptase-positive mast cells were identified intraepithelially and in the lamina propria. In the lamina propria, tryptase staining was observed within mast cells but also outside the mast cells. The staining outside the mast cells, indicating mast cell degranulation, was observed particularly in the IBS comorbid and IBS multicomorbid groups.

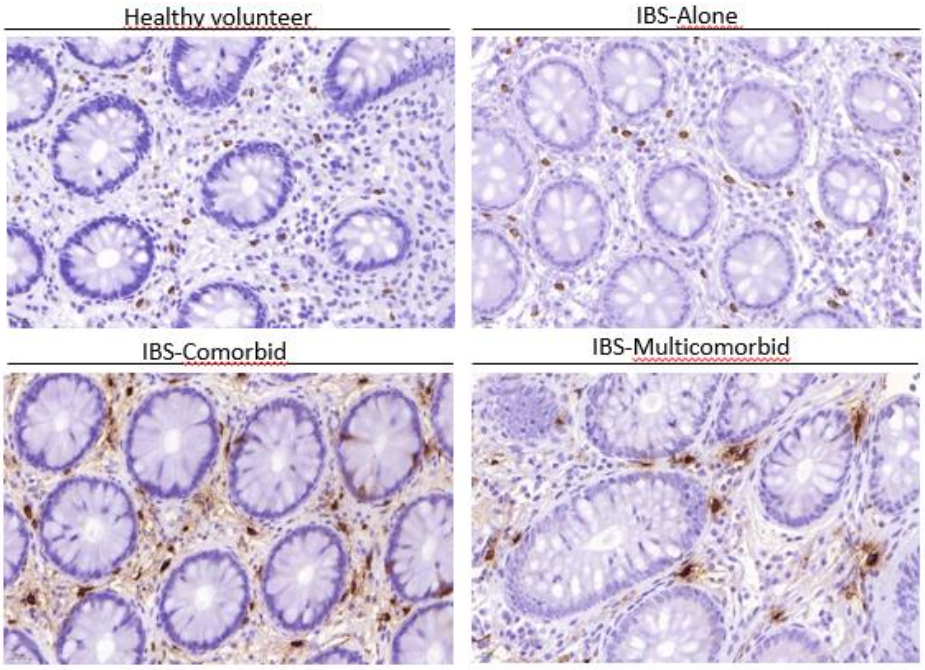

Figure 7 - Representative images of IHC tryptase staining.400x magnification

Epithelium and Lamina propria tryptase positive mast cell count

The number of tryptase positive mast cells was assessed both in the epithelium and lamina propria of HV, IBS-Alone, IBS-Comorbid and IBS-multicomorbid participants. In the epithelium, no significant differences in tryptase positive mast cells per hpf were detected in HV compared to IBS subgroups and also between IBS subgroups. (Figure 7A). Likewise, in the lamina propria, no significant differences in tryptase positive mast cells per hpf were found in HV compared to IBS subgroups and also between IBS subgroups (Figure 7B).

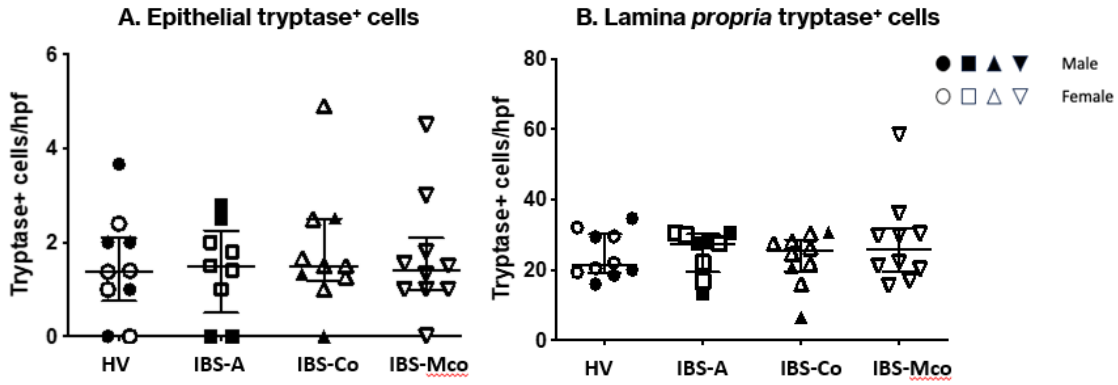

Figure 8 - Tryptase positive mast cell count in the epithelium (A) and lamina propria (B).

(A) Number of mast cells per hpf positively stained for tryptase in the epithelium in HV and IBS-Alone, IBS-Comorbid and IBS-Multicomorbid groups (right plot). (B) Number of mast cells per hpf positively stained for tryptase in the lamina *propria* in HV and IBS-A, IBS-C and IBS-M subgroups. HV: healthy volunteer, IBS-A: IBS alone, IBS-Co: IBS comorbid, IBS-Mco: IBS multicomorbid.

Quantification of tryptase+ stained area in lamina propria

Tryptase$^+$ stained area was quantified in the lamina propria of HV (n=9), IBS-Alone (n=9), IBS-Comorbid (n=10), and IBS-multicomorbid (n=9) individuals. No significant differences in percentage of tryptase$^+$ stained area of the lamina propria were detected in HV compared to IBS subgroups, IBS-Alone, IBS-Comorbid and IBS-multicomorbid. However, tryptase+ stained area in IBS-Comorbid and IBS-multicomorbid was significantly higher compared to IBS-Alone (p=0.038; p= 0.021, respectively) (Figure 8).

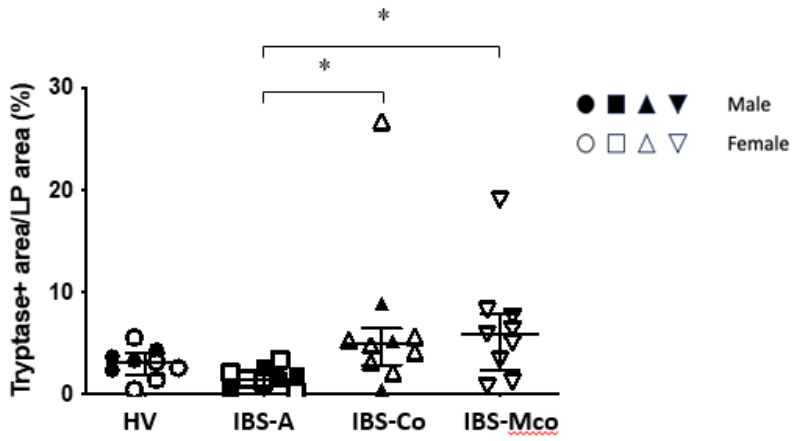

Figure 9 - Tryptase+ staining in the lamina propria.

Area positively stained for tryptase on the lamina *propria* HV and IBS-Alone, IBS-Comorbid and IBS-Multicomorbid. Kruskal-Wallis test and Dunn's multiple comparison test. *p<0.05. HV: healthy volunteer, IBS-A: IBS alone, IBS-Co: IBS comorbid, IBS-Mco: IBS multicomorbid.

4.1.3 Ultrastructural characterization of the intestinal mucosa

At VHIR, the ultrastructure of mast cells from colon biopsies was examined by transmission electron microscopy (TEM) in order to study the morphology of MC granules, the number of granules per area of cytoplasm, the degranulation profile of MC and their activation status, and the distances from MC to nerve fibres.

A. Ultrastructure Methodology.

Biopsies were immersed in conventional fixative solution: 2.5% glutaraldehyde (v/v) (electron microscopy grade, Merck), 2% paraformaldehyde (PFA) (w/v) in 0.1M Phosphate buffer (PB) (pH 7.4) for at least 48 hours at RT. When samples are to be stored more than 48 h, it is convenient to transfer them into a maintenance solution: 1% PFA in 0.1M PB during a maximum of 1 month at 4ºC. Fixed samples were dehydrated and embedded in Epon's resin. After polymerization, all colon samples were cut in ultrathin (70-90 nm) sections with a Leica Ultracut UCT microtome (Leica Micro-systems GmbH). Ultrathin sections were placed on gold grids (100mesh) with a film layer and examined using a TEM JEM-1400 (Jeol Ltd., Tokyo, Japan) equipped with a CCD Gatan ES1000 W Erlangshen camera. Post-fixed sample procedures and sample observation were performed at the Servei de Microscopia of Universitat Autònoma de Barcelona (Bellaterra). Sections from the descending sigmoid region of the colon of HV (n=4), IBS-A (n=5), IBS-Co (n=5) and IBS-Mco (n=5) participants were visualized by TEM to perform

ultrastructure analysis of lamina propria mast cells. A minimum number of 5 mast cells were observed in all the participants.

B. Ultrastructure Results.

Granule morphology

Different granule morphology could be observed along the samples, with scroll pattern, eccentric electron dense core pattern and particle pattern the main granule morphologies observed. Scroll pattern granules are curved, straight or parallel and the centre of the structure can be empty or filled (Figure 9). There are dense compact granules that present an eccentric electron dense core pattern (Figure 9). Moreover, mast cells containing granular particles (Figure 9) were also observed. Through a qualitative analysis, it was observed that along healthy volunteers the eccentric electron dense core inside the granule was the predominant pattern, while in the IBS groups (IBS Alone, IBS-Comorbid and IBS-multicomorbid), the scroll pattern was observed in higher frequency than any other pattern.

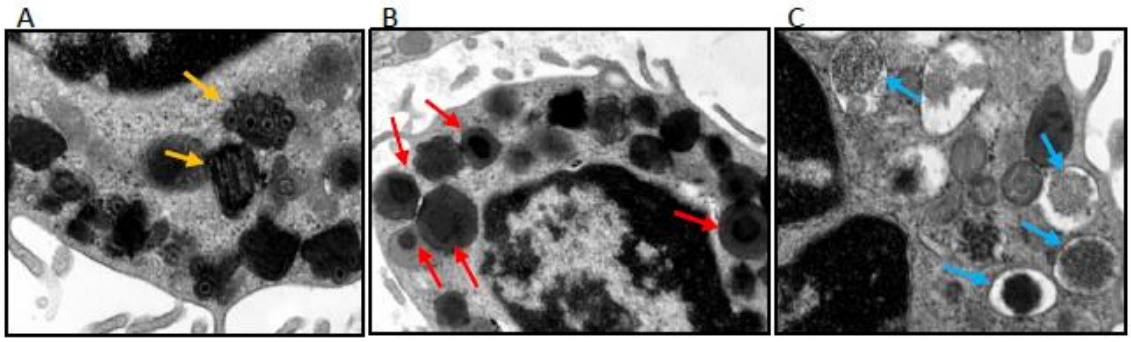

Figure 10 - Granule morphology on colonic mast cells.

(A) Scroll pattern, with central homogeneously electron-dense material (yellow arrows). (B) Eccentric electron dense core pattern (red arrows). (C) Granular particle granules pattern (blue arrows).

Degranulation profile and state of activation

Degranulation of mast cells was also analysed at the ultrastructural level. Mast cell degranulation was observed in all the samples, however within the same sample, mast

cells show different degrees and types of degranulation. Resting mast cells, with no altered granules, were observed along the different groups studied (Figure 10A). Piecemeal degranulation, a vesicle-mediated release of granule contents was observed as a loss of electro-density of the content within the granule. This type of degranulation was observed in almost all the samples. Depending on the degree of piecemeal degranulation we classified mast cells between low medium activation (Figure 10B) and high activation (Figure 10C). Membrane fusion of secretory vesicles together with piecemeal degranulation was also present in several samples (Figure 10D) and mast cells presenting this type of degranulation were classified as very high activation mast cells. Using these mechanisms, the mast cell controls the release of the mediators stored in its cytoplasmic granules.

The four categories of activation (resting, low-medium activation, high activation and very high activation) were observed in all study groups. The different mast cells were included in each category based on visual exploration of the TEM images. Figure 11 shows the percentage of mast cells displaying each degranulation profile in all study groups.

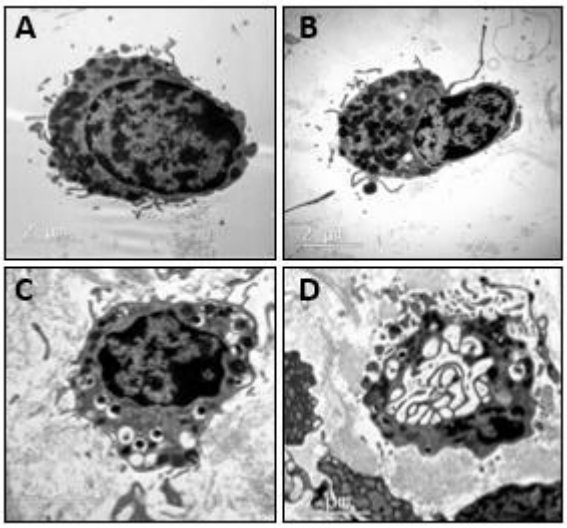

Figure 11 - Ultrastructural micrograph of mucosal degranulated mast cells.

(A) Resting mast cell: no degranulation signs can be observed. All the granules are unaltered. (B) Mast cell undergoing low-medium piecemeal degree degranulation, classified as low-medium activated mast cell. Few-moderate granules are degranulated. (C) Mast cell undergoing high piecemeal degree degranulation, classified as high activated mast cell. Some of the granules are unaltered, but there are many with partially or completely empty granules due to piecemeal degranulation. (D) Mast cell with fusion

of secretory vesicles membrane forming channels and piecemeal degranulation, classified as very high activated mast cell. Magnification: 15000X.

The four categories of activation (resting, low-medium activation, high activation and very high activation) were observed in all study groups. In HV the % of resting MC and the % of low-medium activated MC were significantly higher compared to IBS-Comorbid (p= 0.024) and IBS-multicomorbid groups (p= 0.043), respectively. Moreover, % of low-medium activated MC in IBS-Comorbid was significantly higher compared to IBS-Alone (p= 0.022) and IBS-multicomorbid (p=0.001) groups. IBS-Alone showed a significantly increased % of high activated MC compared to HV (p<0.0001), IBS-Comorbid (p=0.0002) and IBS-multicomorbid (p=0.004) groups. IBS-M showed a significantly increased % of very high activated MC compared to HV (p=0.009) and IBS-A (p=0.031) groups (Figure 11).

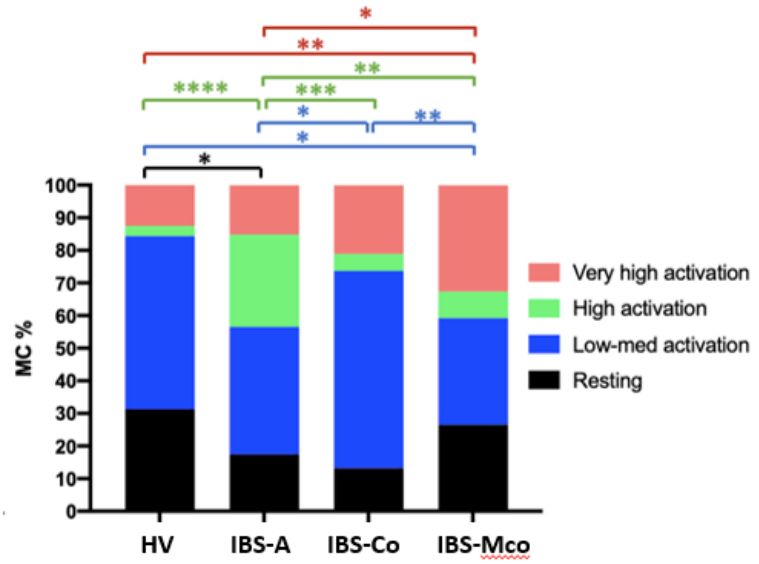

Figure 12 - Percentage of MCs showing differing activation states (no signs of activation (resting), low medium activation, high activation, and very high activation) out of total MC count.

Percentage of HV mast cell with different degrees of activation compared to IBS-Alone, IBS-Comorbid and IBS-multicomorbid groups. MC: mast cell, HV: healthy volunteer, IBS-A: IBS alone, IBS-Co: IBS comorbid, IBS-Mco: IBS multicomorbid. ****p<0.0001, ***p< 0.001, **p<0.01, *p<0.05.

Mast cell-nerve interaction

Both, IBS-comordid and IBS-multicomorbid groups (p=0.013 in both cases) showed increased percentage of MC located <5 µm away from nerve fibres compared to HV, (p=0.0134 in both cases). However, no significant differences were observed between IBS-Alone and HV. (**Figure 12**).

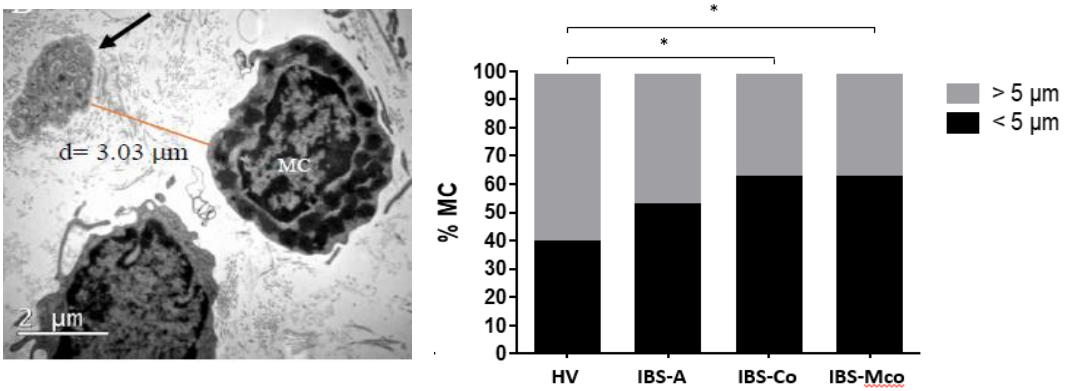

Figure 13 - Percentage of MC located <5 µm and >5 µm away from nerve fibres out of total MC count.
IBS-A (n=6), IBS-Co (n=5) and IBS-Mco (n=5) group (n= 16). MC: mast cell, HV: healthy volunteer, IBS-A: IBS alone, IBS-Co: IBS comorbid, IBS-Mco: IBS multicomorbid. Chi-squared analysis *p<0.05.

5.2 TASK 3.4) Immune, neural and luminal-derived mechanisms of epithelial dysfunction (UNIBO, VHIR, UGOT, KUL, UM).

In order to assess immune, neural and luminal-derived mechanisms of epithelial dysfunction, at UNIBO we used an in vitro model of permeability based on Caco-2 cells to test the effect of mediators spontaneously released by colonic biopsies (called supernatants) collected by WP2.

A. Methodology of in vitro model of permeability based on Caco-2 cells

The human intestinal epithelial cell line Caco-2 was used as an *in vitro* model of the intestinal epithelial barrier. Cells were seeded on porous filters (12-well Transwell Clear, 0.40 µm porosity, 1.1 cm of diameter), at a density of 200.000 cells/filter and cultured in

Dulbecco's modified Eagle's medium (DMEM) (4.5 g/l glucose) supplemented with 2 mmol/l L-glutamine, 50 IU/ml penicillin, 50 μg/ml streptomycin and 10% heat-inactivated fetal bovine serum (FBS) at 37°C and 5% of CO_2.

The culture medium was changed every 2 days. Transepithelial cell resistance (TER) was measured every two days in order to follow the formation and differentiation of the Caco-2 monolayer, using a volt-ohm meter (Millicel® ERS-2 Millipore). Once the monolayer was formed (approximately 14 days after seeding), supernatants were added to Caco-2 cells and changes in paracellular permeability were assessed by measuring the passage of a probe (Fluorescein-5-(and-6)-Sulfonic Acid, FITC) through the Caco-2 monolayer over time. Absorbance measurements were performed at time 0 (immediately after the addition of treatments), every 30 min for the first 2 h, and then every hour for the next 4 h. The FITC absorbance values obtained were directly proportional to permeability change of cell monolayer. Ancillary experiments were performed to determine the incubation time of the supernatant treatments, which was found to be 6 hours.

A. Results of in vitro model of permeability based on Caco-2 cells

IBS supernatants significantly increased Caco-2 permeability, regardless of the presence of comorbidities, (Fig.13A). Interestingly, if we stratify the data according to the recruiting center (Fig. 13B-D), except for KUL, where the number of samples analysed was too small, we found some interesting differences that will be important to evaluate according to clinical and dietary information

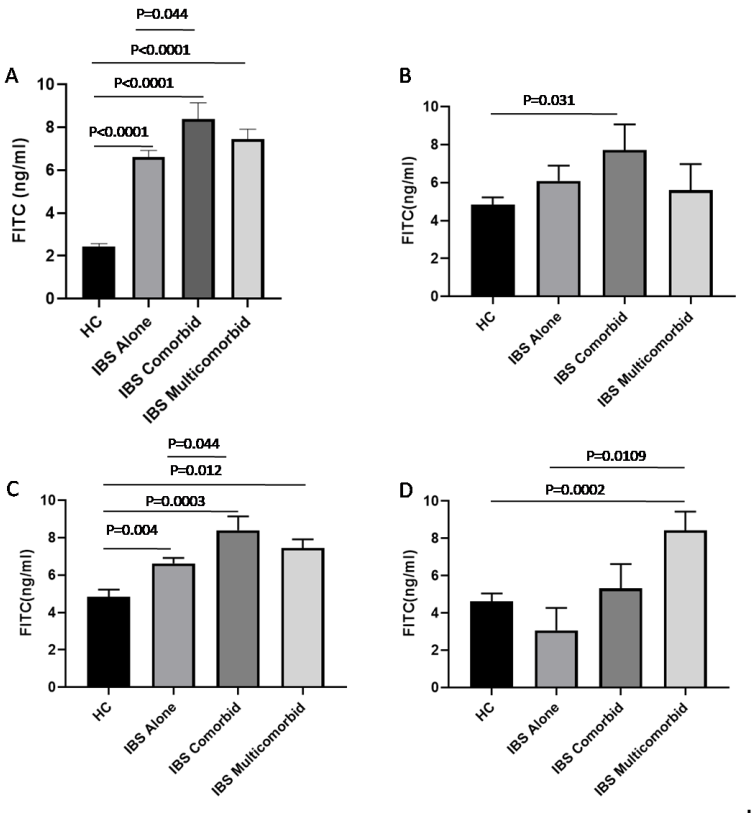

Figure 14 - Effect of mucosal mediators spontaneously released by IBS biopsies on Caco-2 cells.

A: overall effect of received supernatants from UGOT, UNIBO, VHIR and KUL. B: effect of supernatants received from UGOT. HC: 8, IBS alone: 8, IBS comorbid: 9, IBS multicomorbid: 6. C: effect of supernatants received from UNIBO. HC: 7, IBS alone: 12, IBS comorbid: 11, IBS multicomorbid: 4. D: effect of supernatants received from VHIR. HC: 11, IBS alone: 5, IBS comorbid: 4, IBS multicomorbid: 8.

To elucidate the molecular mechanisms underlying the permeability changes induced by IBS supernatants, we extracted RNA from Caco-2 cells to evaluate the gene expression of Tight junctions (TJs) by qPCR. In particular we focused on zonula occludens-1 (ZO-1), occludin and junctional adhesion molecule-A (JAM-A). ZO-1 expression was significantly

reduced in Caco-2 cells incubated with IBS alone and IBS multicomorbid supernatants (Fig. 14A). JAM-A was reduced in Caco-2 cells incubated with all IBS supernatants, while occludin expression was slightly increased by IBS alone and IBS comorbid supernatants, although none of these comparisons reached the statistical significance (Fig. 14B-C).

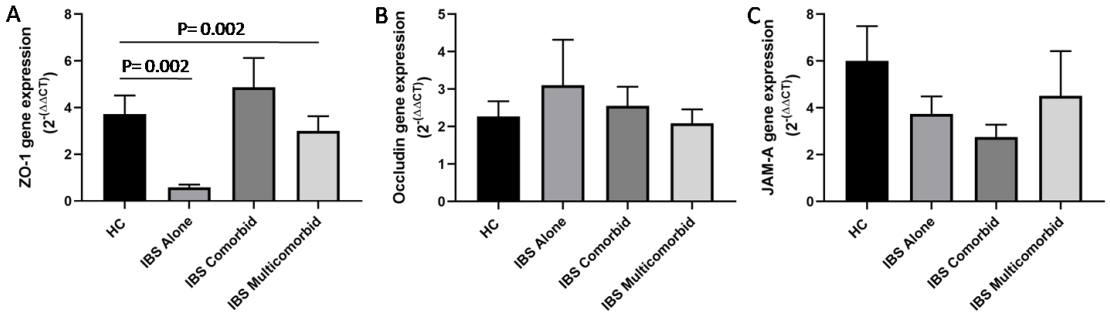

Figure 15 - Tight junction gene expression in Caco-2 cells treated with IBS supernatants.

A: ZO-1 gene expression. HC: 30, IBS alone: 27, IBS comorbid: 25, IBS multicomorbid: 19. B: Occludin gene expression. HC: 23, IBS alone: 27, IBS comorbid: 25, IBS multicomorbid: 19. C: JAM-A gene expression. HC: 23, IBS alone: 27, IBS comorbid: 25, IBS multicomorbid: 19. Results are reported as relative expression ($2^{-\Delta\Delta Ct}$), calibrator group: HC.

Taken together, these data suggest that IBS supernatants increase Caco-2 permeability, at least in part, by affecting the expression of TJs. We then decided to look at the gene and protein expression of TJs in the biopsies corresponding to the supernatants used to treat Caco-2 cells. We found that both gene (Fig.15 A-C) and protein (Fig.15 D-F) expression was altered in IBS compared to controls, although these experiments are still ongoing.

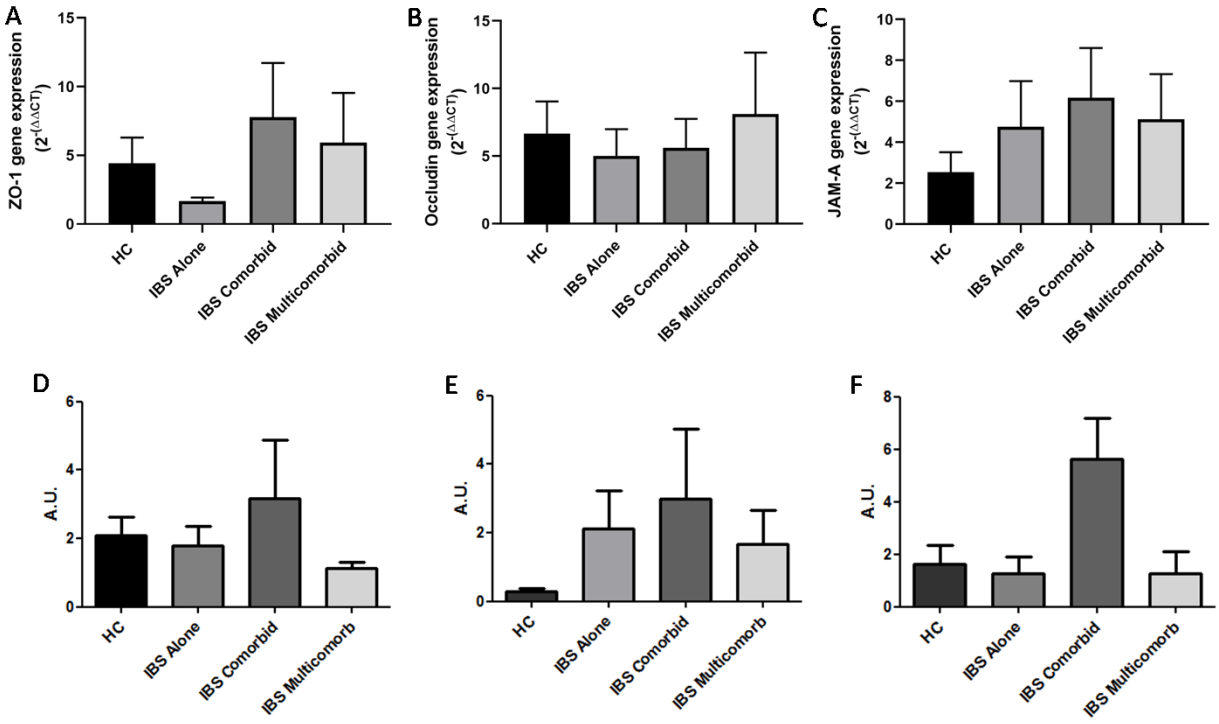

Figure 16 - Tight junction gene and protein expression in HC and IBS colonic biopsies.

A: ZO-1 gene expression. B: Occludin gene expression. C: JAM-A gene expression. HC: 23, IBS alone: 27, IBS comorbid: 25, IBS multicomorbid: 19. Results are reported as relative expression ($2^{-\Delta\Delta Ct}$), calibrator group: HC. D: ZO-1 protein expression. E: Occludin protein expression. E: JAM-A protein expression. HC: 6, IBS alone: 6, IBS comorbid: 5, IBS multicomorbid: 5.

To assess the effect of plasma samples on Caco-2 permeability, we performed preliminary experiments to evaluate the effect of two different dilutions on the pH of the Caco-2 growth medium and on Caco-2 vitality. Based on these results we carried out the next experiments for 24h, adding the plasma samples diluted 1:100 on the basolateral side.

To evaluate the effect of IBS supernatants on neurons after the induction of barrier dysfunction, we set up co-culture experiments using Caco-2 cells and a neuronal cell line (SH-SY-5Y). In the transwelll plate, the SH-SY5Y were seeded on the basolateral side, while the supernatants were added on the apical side, in contact with the Caco-2 cells. In order to obtain live-cell imaging, we performed these experiments in the Incucyte, which has the advantage of obtaining images over time while the cells are stable in the incubator. We tried different incubation times and images acquisition times to identify the best experimental conditions.

4. CONCLUSIONS

In this deliverable we describe the work performed so far with mucosal biopsies collected from subjects recruited in WP2 to characterize the molecular, cellular and ultrastructural profile in IBS patients and IBS patients with associated mental and somatic comorbidities. Transcriptomic and proteomic analysis of colonic biopsies revealed several proteins differentially expressed between IBS and IBS associated to mental and somatic comorbidities suggesting a different molecular profile between these groups. Cellular characterization through immunohistochemistry analysis unveiled an increase in GAP43 positive fibres in IBS comorbid and multicomorbid groups. Ultrastructural analysis also showed a higher mast cell degranulation in these groups compared to healthy controls.

These results suggest that mental and somatic comorbidities in IBS patients are associated with different molecular, cellular and ultrastructural profiles. However, validation experiments need to be performed to confirm these results.

5. REFERENCES

[1] Martínez C, González-Castro A, Vicario M, Santos J. Cellular and molecular basis of intestinal barrier dysfunction in the irritable bowel syndrome. Gut Liver. 2012 Jul;6(3):305-15.

[2] Acciarino A, Diwakarla S, Handreck J, Bergola C, Sahakian L, McQuade RM. The role of the gastrointestinal barrier in obesity-associated systemic inflammation. Obes Rev. 2024 Mar;25(3):e13673.

[3] Poto R, Fusco W, Rinninella E, Cintoni M, Kaitsas F, Raoul P, Caruso C, Mele MC, Varricchi G, Gasbarrini A, Cammarota G, Ianiro G. The Role of Gut Microbiota and Leaky Gut in the Pathogenesis of Food Allergy. Nutrients. 2023 Dec 27;16(1):92.

[4] Makris AP, Karianaki M, Tsamis KI, Paschou SA. The role of the gut-brain axis in depression: endocrine, neural, and immune pathways. Hormones (Athens). 2021 Mar;20(1):1-12.

[5] Martín F, Blanco-Suárez M, Zambrano P, Cáceres O, Almirall M, Alegre-Martín J, Lobo B, González-Castro AM, Santos J, Domingo JC, Jurek J, Castro-Marrero J. Increased gut permeability and bacterial translocation are associated with fibromyalgia and myalgic encephalomyelitis/chronic fatigue syndrome: implications for disease-related biomarker discovery. Front Immunol. 2023 Sep 7;14:1253121.

[6] Love, M. I., Huber, W., & Anders, S. (2014). Moderated estimation of fold change and dispersion for RNA-seq data with DESeq2. *Genome biology*, *15*, 1-21.

[7] Ritchie, M. E., Phipson, B., Wu, D. I., Hu, Y., Law, C. W., Shi, W., & Smyth, G. K. (2015). limma powers differential expression analyses for RNA-sequencing and microarray studies. *Nucleic acids research*, *43*(7), e47-e47.